Ab initio studies of structural and mechanical properties of NH3, NO and N2O hydrates

Ningru Sun[1], Nianxiang Qiu[2], Yanjun Li[1], Siguang Li[1], Longbin Yang[1], Kan Luo[2], and Shiyu Du[3]

[1]Haerbin Engineering University
[2]Ningbo Institute of Industrial Technology Chinese Academy of Sciences
[3]Chinese Academy of Sciences

May 5, 2020

Abstract

The mechanical properties play a vital role in the stability and behavior of clathrate hydrate. In this work, the structural and mechanical properties of some nitride gas (NH3, NO and N2O) hydrates were investigated using density functional theory calculations. The equilibrium lattice structures for these hydrates were obtained. The full second-order elastic constants were then determined by energy–strain analyses and the polycrystalline elastic properties were also predicted. It is found that these three gas hydrates have high elastic isotropy, but their shear properties are significantly different. This study may lay a theoretical foundation for future research on the structural evolution of clathrate hydrates under a mechanical field.

1.INTRODUCTION

The 21st century is the era when the traditional fossil energy is being replaced by clean energy.[1, 2] Clathrate hydrates (hereinafter referred to as "hydrates" when no misleading) are non-stoichiometric crystalline inclusion compounds that can form under low temperatures or high pressures conditions and can exist both above and below the freezing point of water.[3, 4] More than 130 guest compounds are known to form hydrates with water molecules and are typically hydrophobic natural gases such as CH_4 and CO_2.[5] Hydrates are of interest to the public due to the well known natural gas hydrates. Their formation requires relatively low temperature and high pressure.[1] There are three common types of gas hydrate structures: sI, sII, and sH hydrates. In the environment, gas hydrates are mainly of the sI and sII types. sH hydrates are also confirmed to exist in nature, such as in the Gulf of Mexico and Cascadia Margin.[6-8] Although other structural types such as sT type and half-clathrate hydrates were also reported,[9-11] so far they exist only in the laboratory. In the mid 1960s and early 1980s large reservoirs of gas hydrates were found in permafrost and marine areas, respectively,[12, 13] by governments, as well as oil and gas companies. This raised the interest in exploitation and application related activities from all walks of life, especially the academic community. For hydrates as an energy resource, their stability needs to be addressed thoroughly for the correspondence to global climate change since methane is an important greenhouse gas. Therefore, a growing number of investigations on natural gas hydrates have been conducted, and the research contents have expanded from the initial flow assurance for preventing blocking of oil and gas pipelines[14, 15]to resource potential,[16-18] safe drilling,[19] geological hazards,[20, 21] the carbon cycle,[22] climatic change,[23, 24] and even outer space hydrates.[25]

Due to the massive emissions of greenhouse gases that have caused the global warming, scholars have proposed the capture and storage (CCS) of greenhouse gases.[26] Under this storage technology, the replacement of CH_4 with CO_2 from natural gas hydrates has been demonstrated to be possible from both experimental and theoretical investigations. Considering the complication in geology as well as exploitation conditions for

the practice of CCS with natural gas hydrates, it is necessary to determine the elasticity and mechanical strength of the generated greenhouse gas hydrate membrane.[27] Moreover, this also provides requisite data in future hydrate technology to design the structures, shapes and sizes of the transport systems according to the mechanical strength of solid hydrate.[28] Up to now, exploration on hydrate mining and replacement is concentrated to CO_2 and organic gases, and only limited works have been carried out on the remaining greenhouse gases, which were found have the potential to extract natural gas from hydrates in the previous work.[29] Therefore, it is crucial to find the mechanical properties for different greenhouse gas components, such as nitrogen-containing small molecules, encapsulated in clathrate hydrates.

With the development of super computing technology, theoretical calculations have been recognized as a powerful scheme that can provide critical insight and understanding of the structure and properties of gas hydrates. In recent decades, several properties of gas hydrates have been predicted in theory including the structures, thermodynamic stability, nucleation and growth processes, grain size and grain mechanics. For example, *Rey et al.* used density functional theory (DFT) to study the mechanical properties and structures of methane and carbon dioxide hydrate, which shows that the two gas hydrates are both highly isotropic, but they differ significantly in shear properties.[30] *English et al.*carried out molecular dynamics (MD) simulations to analyze the dynamic properties of sI H_2S hydrate.[31] *Zeina et al* calculated the elastic mechanical parameters of methane hydrate using the first principle method, and the obtained results agree well with the previous experimental data[32]. *Uchida et al.* used MD simulation to calculate the bulk elastic modulus of hydrates in different ratios of CH_4 and CO_2.[33, 34] In our previous works, we have studied the structure and formation mechanisms of clathrate hydrates encaging different gases[34] and the structures and mechanical properties of CH_4, SO_2, and H_2S hydrates were investigated with DFT.[35] Recently, the occupancy isotherms of pure CH_4, pure CO_2 and their mixture in sI and sII hydrates are studied by our group using grand canonical Monte Carlo and molecular dynamics hybrid (GCMC+MD) simulations. We have shown that the mixing of CO_2 into CH_4 may have stabilization effect on sI hydrate, providing a thermodynamic basis for the feasibility of CO_2 to promote CH_4mining.[36] Then the adsorption behavior and phase equilibrium for clathrate hydrates of sulfur- and nitrogen-containing small molecules were also predicted. We found that the SO_2, H_2S, N_2O, and even CS_2 gases have the ability to replace the CH_4 gas from natural gas hydrates. Results from that study suggest that some components in flue gases may assist the displacement of CH_4. This implies that one may save significant effort in separation of different components from flue gases when performing replacement of CH_4 gas in natural gas hydrates with CO_2.[29, 36]

Up to now, investigations on structures and properties for some hydrates like CO_2, H_2S and SO_2hydrates[35, 37] have been performed, but only a few inspections have been conducted on mechanical properties of hydrates encaging nitrogen-containing small molecules. This article presents a computational study on the elastic constant tensor of nitrogen-containing small molecules hydrates from DFT. This work seeks to shed a light on the differences in elastic mechanical properties of three hydrates and their impact on hydrates' behavior.

2. METHODOLGY

2.1. Structure generation

The NO, N_2O and NH_3 are sufficiently small molecules to form hydrates in the sI structure under certain pressure–temperature conditions.[5] The primitive lattice unit consists of two 5^{12} cages with 12 pentagonal faces, and six $5^{12}6^2$cages with 12 pentagonal and 2 hexagonal faces, totally 46 water molecules.[38] In the initial guesses, the structures for these three hydrates were based on high-resolution neutron diffraction data for deuterated methane hydrates, the hydrogen atoms are disordered just like those in the ice Ih structure and their positions were assigned randomly but in accordance with the Bernal–Fowler ice rules.[5] The cage occupancy was assumed to be 100% with a guest gas molecule at the center of every cage.

2.2. Full elasticity tensor determination

In this work, we first determined the equilibrium cell parameters for the stress-free states. Then full sets of second order elastic constants (SOECs) were calculated using the homogeneous finite strain method incorporated with the first-principle total energy method. The detailed description of this method can be

found in the early publication.[39] In short, elastic constants are defined by expanding the Gibbs free energy as a Taylor series versus Lagrangian strains. The second-order Taylor expansion coefficients as combinations of SOECs of the crystal are obtained from a polynomial fit to the calculated energy-strain relation. Using SOECs, the bulk modulus (B) and shear modulus (G) of the clathrate hydrate crystals are calculated via the Voigt-Reuss-Hill averaging scheme.[40] Afterwards, (E) and Poisson's ratio (v) can be calculated from B and G .

The sI hydrate structure is cubic, thus, three independent elastic constants c_{11}, c_{12}, and c_{44} are required which can be determined from three Lagrangian strains e_1, e_2, and e_3. Though a stress strain analysis could have been applied, an energy strain analysis is believed to be preferable.[41] The total energy variation of the system can be expanded as a Taylor series of the elastic strain.[42, 43] For a system at zero pressure, one has

$$\Delta E = \frac{v}{2} \sum_{i=1}^{6} \sum_{j=1}^{6} c_{ij} e_i e_j + O(e_i^3) \ (1)$$

Here V is the volume of the undistorted lattice cell at which the ionic positions were fully optimized, ΔE is the energy change resulting from the strain vector e = (e_1, e_2, e_3, e_4, e_5, e_6) in Voigt notation, and c_{ij} is the matrix elements of elastic constants. The primitive lattice vectors a_i (i = 1...3) of a crystal are transformed to the new vectors a_i ' under the strain by

$$\begin{pmatrix} a_1' \\ a_2' \\ a_3' \end{pmatrix} =$$

$$\begin{pmatrix} a_1 \\ a_2 \\ a_3 \end{pmatrix} \bullet (+\varepsilon) \ (2)$$

Where ε is the strain tensor. It relates to the strain vector e by

$$\varepsilon =$$

$$\begin{pmatrix} e_1 & \frac{e_6}{2} & \frac{e_5}{2} \\ \frac{e_6}{2} & e_2 & \frac{e_4}{2} \\ \frac{e_5}{2} & \frac{e_4}{2} & e_3 \end{pmatrix} \ (3)$$

Three modes corresponding to three different sets of small strains were used. A volume-conserving tetragonal strain e = (δ ,-δ ,δ^2/(1-δ^2),0,0,0) was applied according to Equation (3) yields:

$$\Delta E = V(c_{11} - c_{12})\delta^2 + O(\delta^4) \ (4)$$

Then the [100] and [010] strain e = (δ,δ,0,0,0,0) was applied which leads to:

$$\Delta E = V(c_{11} + c_{12})\delta^2 + O(\delta^2) \ (5)$$

Last, c_{44} was calculated from the [111] shear strain e = (0,0,0,δ,δ,δ)

$$\Delta E = \frac{3V}{2} c_{44} + O(\delta^2) \ (6)$$

Combining (4), (5), and (6) the relevant elastic constants c_{11}, c_{12}, and c_{44} are obtained by fitting to a polynomial of δ varying from -0.03 to 0.03. Equations of elastic properties are listed in the following.[44]

The bulk modulus (B) can be calculated from:

$$B = \frac{(c_{11}+c_{12})}{3} \ (7)$$

Shear modulus:

$$G_{Reuss} = \frac{5(c_{11}-c_{12})c_{44}}{4c_{44}+3(c_{11}-c_{12})} \ (8)$$

3

$$G_{\text{Voigt}} = \frac{(c_{11} - c_{12} + 3c_{44})}{5} \qquad (9)$$

$$G = \frac{G_{\text{Voigt}} - G_{\text{Reuss}}}{2} \qquad (10)$$

Poisson's ratio:

$$\upsilon = \frac{(\frac{3}{2})B - G}{G + 3B} \qquad (11)$$

Young's modulus:

$$= 2G(1 + \upsilon) \qquad (12)$$

Longitudinal wave speed:

$$V_p = \left(\frac{B + (\frac{4}{3})G}{\rho} \right)^{\frac{1}{2}} \qquad (13)$$

Transverse wave speed:

$$V_s = \left(\frac{G}{\rho} \right)^{\frac{1}{2}} \qquad (14)$$

Zener anisotropy ratio:

$$A_Z = \frac{2c_{44}}{c_{11} - c_{12}} \qquad (15)$$

3. RESULTS AND DISCUSSIONS

3.1 Structures

All first-principles calculations are carried out by the CASTEP program under the Material Studio 7.0 version.[45] The energy cutoff is 400 eV. The ultrasoft form pseudopotentials are utilized in the calculations. The convergence criteria of energy, maximum force, maximum stress, and maximum displacement were set as 5.0×10^{-6} eV/atom, 0.01 eV Å^{-1}, 0.02 Gpa, and 5.0×10^{-4} Å, respectively, for optimization. In our previous work, generalized gradient approximation (GGA) with the revised Perdew-Burke-Ernerhorf (revPBE) and the Perdew-Burke-Ernerhorf (PBE) functionals have been used to calculate the equilibrium lattice parameters of methane hydrates. Comparing the results with previous ones and the experimental value, the prediction from revPBE is found closer to the experimental measurement and other theoretical works[35]. Therefore, revPBE functional is adopted in the following calculations in this work. Here, we calculated three type sI clathrate hydrates, i.e., NH_3 hydrates and N_2O hydrates and NO hydrates, all the crystalline structures are plotted in **Figure 1** . The lattice parameters by the equations of state (EOS) fitting,[46] and the fitting curve of Energy vs. Volume for NH_3, N_2O and NO hydrates are shown in **Figure 2** . The predicted lattice parameters for NH_3, NO and N_2O hydrates are 12.095, 12.126 and 12.36 Å, respectively, higher than the value for the CH_4 hydrate(11.955 Å).[47] The lattice parameters of the N_2O hydrate can be found to be larger than those of NO and NH_3 mainly because N_2O has a larger diameter. It is interesting to further study the bulk modulus in terms of the attractive and repulsive interatomic interactions and the type of occupied cage.
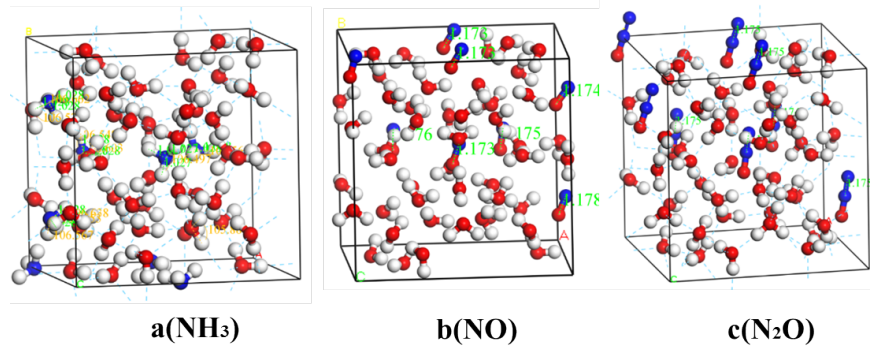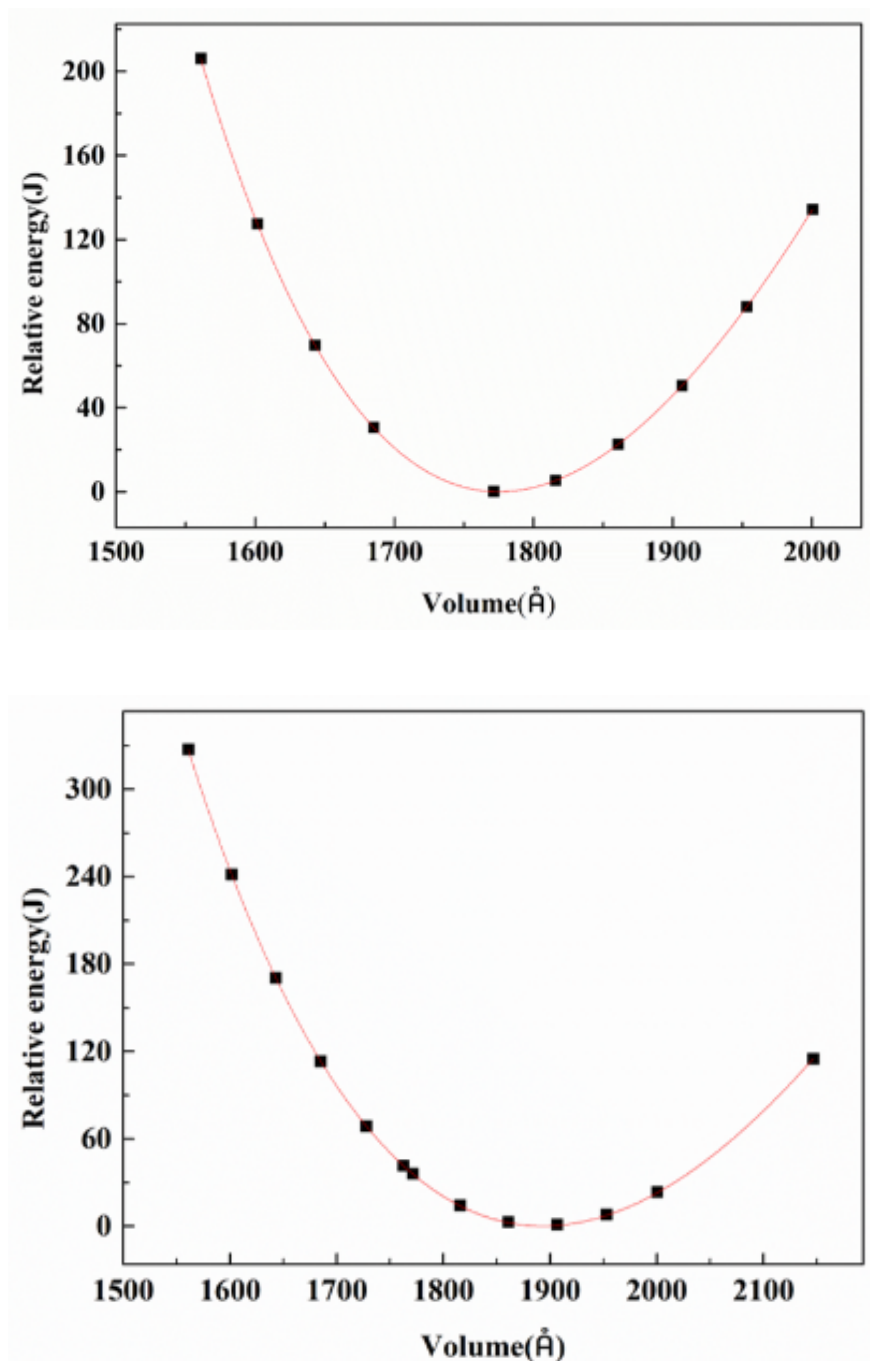

a(NH₃)　　　　**b(NO)**　　　　**c(N₂O)**

Figure 1. Crystal structures for NH$_3$ hydrate (a), NO hydrate (b) and N$_2$O hydrate (c). Color scheme: red for oxygen, white for hydrogen, and blue for nitrogen.
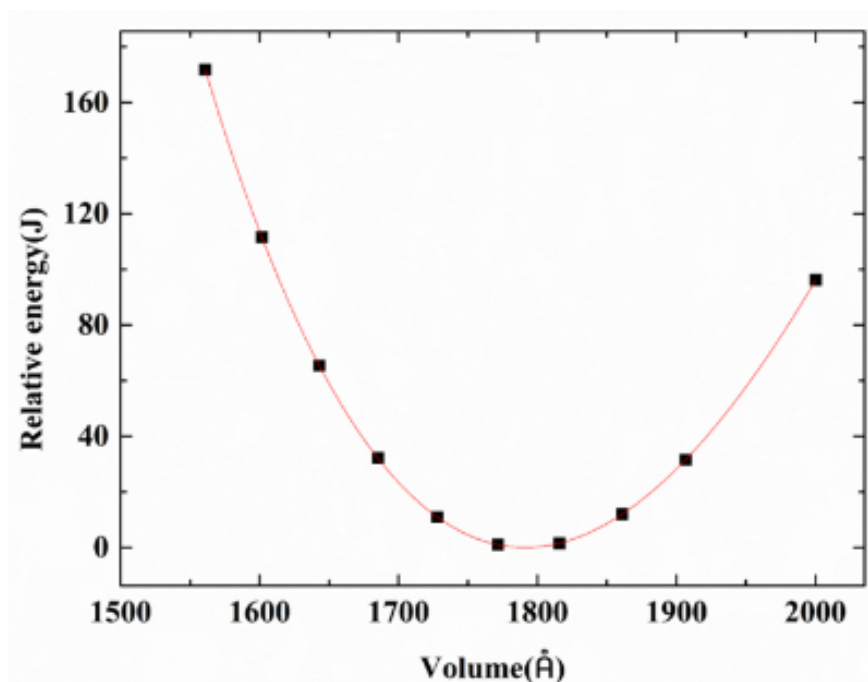
Figure 2 . Energy versus volume curve for NH_3, N_2O and NO hydrates using revPBE XC functional and fitted using Murnaghan equation, respectively.

3.2. Elastic properties

The theoretical prediction of the elastic mechanical properties of NH_3, NO and N_2O hydrates are carried out in this work. To the authors' knowledge, this is the first time that the sI crystalline structures of NH_3, N_2O and NO hydrates have been studied with DFT. The calculation results for single-crystal SOEC are given in **Table 1** and all energy-strain curves are shown in **Figure 3** for NH_3, N_2O and NO hydrates with 100From**Table 1** , the N_2O hydrate is found to have a slightly lower bulk modulus than the methane hydrate. Unlike nitrous oxide, hydrogen atoms in methane molecules are more likely to generate hydrogen bonds with water molecules aligned in a tetrahedron pattern, which may increase the rigidity of the skeleton between guest molecules and water molecules. The NH_3 and NO hydrates have a slightly higher bulk modulus than the methane hydrate as **Table 1** shows. On the one hand, higher B for NH_3 can be attributed to three hydrogen atoms per molecule that facilitate the formation of multiple hydrogen bonds to the water molecules and NO is a polar molecule that adds to the intermolecular interactions with the water molecules; on the other hand, unlike methane, nitrogen atoms in ammonia and nitric oxide are more electronegative compared with carbon atoms in methane.

On the whole, the characteristics of the three hydrates are similar in most respects with N_2O showing a higher curvature. All hydrates are almost isotropic as reflected by the Zener anisotropy factor A_Z. A similar observation of isotropy was obtained in the experimental work of *Shimizu et al* .[48] using Brillouin spectroscopy on methane hydrate single crystals. They attributed this isotropy to the void-rich network and departure from the ideal tetrahedral arrangement of oxygen atoms in methane hydrates. In addition to these reasons, we believe that the randomness of the hydrogen positions in the cubic lattice may contribute to this isotropy. The slightly lower isotropy of nitrous oxide hydrates in this work may be due to the geometry or bond orientation in nitrous oxide molecules.

The SOEC of N_2O has large difference relative to those of methane hydrate, especially c_{12} and c_{44}. The polarity of this molecule may be a reason since it induces stronger hydrogen bonding between host and guest molecules than methane, which can be more susceptible to structural deformation and results in a significant

impact on the elastic constants. As a result, the Bulk and shear modulus differ significantly between methane and N_2O hydrates. The shape of the N_2O molecule and its interaction with the host water molecules might also explain this. From the geometric perspective, the ratio of molecular diameter to cage diameter is larger for N_2O hydrate than methane hydrate, which enhances the stiffness of the hydrate. Interestingly, the NH_3 hydrate is predicted to be closer to the methane hydrate in both elastic constants as well as mechanical modulus than NO and N_2O. It is probably because NH_3's interaction with H_2O as both the hydrogen bond donor and acceptor allows more flexibility to adapt to the shear distortion. These demonstrate that the encaged species indeed have significant impact on the mechanical behavior of the hydrates. When a shear strain takes place, it induces stronger hydrogen bonding change between host and guest molecules since NO and N_2O are both highly polar molecules, resulting in a relatively high shear modulus; When tensile strain occurs, hydrogen atoms in CH_4 and NH_3 molecules are more likely to generate hydrogen bonds with hydrogen atoms in water molecules, increasing the intermolecular interaction between guest molecules and water molecules, resulting in a relatively high Poisson's ratio.
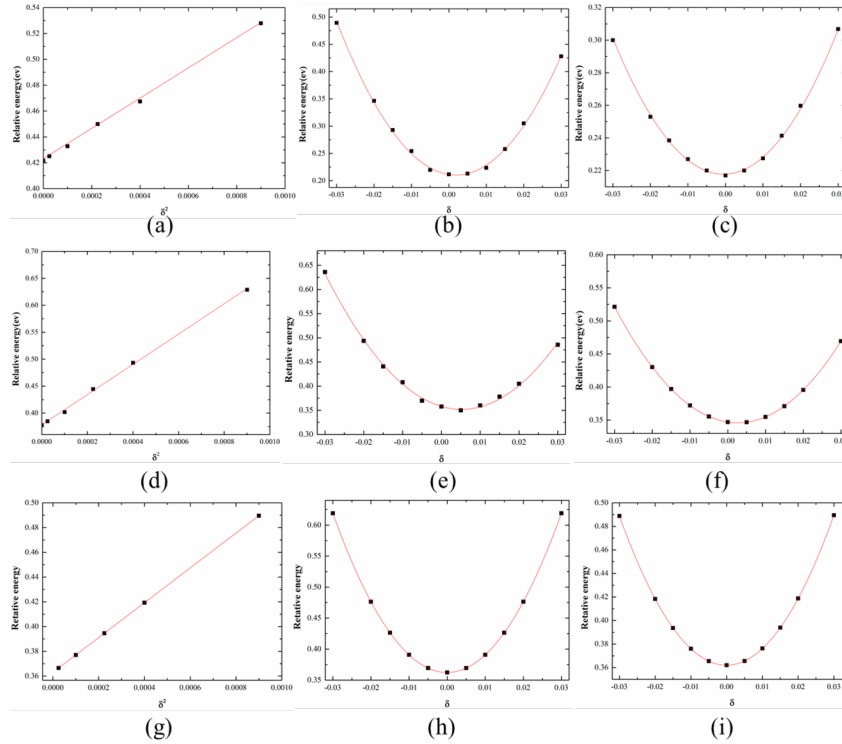

Figure 3 . Strain energy density in volume-conserving tetragonal distortion (a), (d), (g), [100]/[010] strain (b), (e), (h) and shear deformation (c), (f), (i) for NH_3,N_2O,and NO hydrate, respectively .

Table 1 .The predicted elastic constants, density, bulk modulus, shear modulus, Poisson's ratio, Young's modulus, compressional wave speed, and shear speed of NH_3, N_2O and NO hydrates

Elastic parameters	NH_3	NO	N_2O	CH_4[42]
c_{11}/GPa	17.836	19.145	18.465	18.1
c_{12}/GPa	7.247	6.499	1.005	5.7
c_{44}/GPa	5.859	8.464	9.32	6.2
ρ/g cm^{-3}	0.906	1.039	1.035	0.943
B/ GPa	10.777	10.714	6.825	10.40(9.11$^{\mathrm{exp}}$)

Elastic parameters	NH_3	NO	N_2O	CH_4[42]
G/ GPa	5.6261	7.531	9.085	6.23
ν	0.278	0.215	0.039	0.238
E/ GPa	14.380	18.30	18.88	15.4
V_p/Km^{-1}	4.721	4.47	4.278	4.386
V_s/Km^{-1}	2.619	2.39	2.96	2.571
A_z	1.107	1.34	1.068	0.99

It's worth mentioning that temperature and pressure are also important factors affecting hydrates not only because an excessively high temperature or low pressure will result in melting of the hydrates but also because the chemical interaction between gas molecules and water cages might be significantly influenced. Therefore, the study of the mechanical properties of hydrates needs to consider a number of additional factors besides the current theoretical results which will be performed in our future work via simulations in a larger scale in combination with more experimental results in order to build a reliable theory on clathrate hydrates.

4. CNOCLUSION

In this paper, we have presented the DFT calculations of the structures and the second -order elastic parameters for NH_3, N_2O and NO hydrates. Taking into account the difference of the calculation method, and experimental conditions, the calculated mechanical properties of NH_3, N_2O and NO hydrate are analyzed. Although the mechanical properties of NH_3, N_2O and NO hydrates are similar, they are significantly different from those of CH_4hydrate due to the polar nature of these three molecules. The current investigation is expected to further enrich the theory for hydrates and may trigger more theoretical exploration on the physics of hydrates.

ACKNOWLEDGMENTS

References:

1. Chu, S., Majumdar, A. *Nature* **2012** , *488* (7411), 294-303.

2. Du S., Francisco, J. S., Kais, S. *J. Chem. Phys.* **2009** ,*130* (12), 124312.

3. Sloan, E. D. *Nature* **2003** , (426), 353-359.

4. Moon, C., Hawtin, R. W., Rodger, P. M. *Faraday Discuss.* **2007** ,*136* (1), 367-382.

5. Koh, E. D. S. A. Clathrate Hydrates of Natural Gases. CRC Press: Boca Raton,**2008** .

6. Sassen, R., Macdonald, I. R. *Org. Geochem.* **1994** , *23* (6), 1029-1032.

7. Fleischer, E. B., Janda, K. C. *J. Phys. Chem. A* **2013** , *117*(19), 4001-10.

8. Snehanshu., Kundu ., T., K. *J. Chem. Sci.* **2013** , *125* (2), 379-385.

9. Udachin, K. A., Ratcliffe, C. I., Ripmeester, J. A. *Angewandte Chemie International Edition* **2010** , *40* (7), 1303-1305.

10. Chapoy, A., Anderson, R., Tohidi, B. *J. Am. Chem. Soc.* **2007** ,*129* (4), 746.

11. Shin, K., Kim, Y., Strobel, T. A., Prasad, P. S., Sugahara, T., Lee, H., Sloan, E. D., Sum, A. K., Koh, C. A. *J. Phys. Chem. A* **2009** , *113* (23), 6415-6418.

12. Kuznetsov, A. F., Nesterov, A. N. **2001** .

13. Paull, C. K., Ussler, W. I., Borowski, W. S., Spiess, F. N. *Geology* **1995** , *23* (1), 89-92.

14. Dholabhai, P. D., Englezos, P., Kalogerakis, N., Bishnoi, P. R. *Can. J. Chem. Eng.* **1991** , *69* (3), 800-805.

15. Gorman, A. R., Senger, K. *Journal of Geophysical Research Solid Earth* **2010** , *115* (B7), -.

16. Boswell, R., Collett, T. S. *Energ. Environ. Sci.* **2011** , *4* (4), 1206-1215.

17. Boswell, R. *Science* **2009** , *325* (5943), 957-958.

18. Rutqvist, J., Moridis, G. J., Grover, T., Collett, T. *Journal of Petroleum Science & Engineering* **2009** , *67* (1-2), 1-12.

19. Freijayoub, R., Tan, C., Clennell, B., Tohidi, B., Yang, J. *Journal of Petroleum Science & Engineering* **2007** , *57* (1), 209-220.

20. Sultan, N., Cochonat, P., Foucher, J. ., Mienert, J. *Mar. Geol.* **2004** , *213* (1), 379-401.

21. Garziglia, S.; Sultan, N.; Cattaneo, A.; Ker, S.; Marsset, B., Riboulot, V., Voisset, M., Adamy, J., Unterseh, S. Identification of Shear Zones and their Causal Mechanisms Using a Combination of Cone Penetration Tests and Seismic Data in the Eastern Niger Delta. **2010** .

22. Archer, D., Buffett, B., Brovkin, V. *P. Natl. Acad. Sci. Usa.* **2009** , *106* (49), 20596-20601.

23. Xu, W., Lowell, R. P., Peltzer, E. T. *Journal of Geophysical Research Atmospheres* **2001** , *106* (B11), 26413-26423.

24. Schmidt, G. A., Shindell, D. T. *Paleoceanography* **2003** , *18* (1), -.

25. Loveday, J. S., Nelmes, R. J., Guthrie, M., Belmonte, S. A., Allan, D. R., Klug, D. D., Tse, J. S., Handa, Y. P. *Nature* **2001** , *410* (6829), 661-3.

26. Busch, A.; Amann, A.; Kronimus, A.; Kühn, M. Carbon Capture and Storage (Ccs): Overview, Developments, and Challenges. Egu General Assembly Conference, 2010.

27. Uchida, T., Kawabata, J. *Energy* **1997** , *22* (2-3), 357-361.

28. Koh, B. H., Choi, J. H. *Int. J. Precis. Eng. Man.* **2009** , *10* (5), 85-88.

29. Qiu, N., Bai, X., Xu, J., Sun, N., Francisco, J. S., Yang, M., Huang, Q., Du, S. *The Journal of Physical Chemistry C* **2018** .

30. Rey, A. D. *Mol. Simulat.* **2015** , *41* (7), 572-579.

31. English, N. J., Tse, J. S. *J. Phys. Chem. A* **2011** , *115* (23), 6226-32.

32. Jendi, Z. M., Rey, A. D., Servio, P. *Mol. Simulat.* **2014** , *41* (7), 572-579.

33. Uchida, T., Kawabata, J. *Energy* **1997** , *22* (2–3), 357-361.

34. Sun, N., Li, Z., Qiu, N., Yu, X., Zhang, X., Li, Y., Yang, L., Kan, L., Huang, Q., Du, S. *J. Phys. Chem. A* **2017** , *121* (13), 2620-2626.

35. Xinxuan, Z., Guoling, C., Nianxiang, Q., Qing, H., H., J., Shi, D., Yong, F. *Chem. Lett.* **2017** , *46* , 1141-1144.

36. Qiu, N., Bai, X., Sun, N., Yu, X., Yang, L., Li, Y., Yang, M., Huang, Q., Du, S. Hydrates. *J. Phys. Chem. B* **2018** .

37. Nohra, M., Woo, T. K., Alavi, S., Ripmeester, J. A. *J. Chem. Thermodyn.***2012** , *44* (1), 5-12.

38. Steed, J. W.; Atwood, J. L. Supramolecular Chemistry. Wiley: **2009** .

39. Zhao, J., Winey, J. M., Gupta, Y. M. *Physical Review B Condensed Matter***2007** , *75* (75), 4105.

40. Grimvall. Thermophysical Properties of Materials. **1986** .p45

41. Ortega, I., Matanen, A., Kurte, T., Vehkama Ki, H. Computational and Theoretical Chemistry, **2011** , *965* , 353-358.

42.Team,S.GgaPseudopotentialDatabase.http://www.departments.icmab.es/leem/siesta/Databases/index.html.

43. Atom, a Program for Dft Calculations in Atoms and Pseudopotential Generation. Https://Www.Mail-Archive.Com/Siesta-L@Listserv.Uam.Es/Msg04535.Html.

44. Nohra, M., Woo, T. K., Alavi, S., Ripmeester, J. A. *J. Chem. Thermodyn.***2012** , *44* (1), 5-12.

45. CLARK., Stewart, J., SEGAL ., Matthew, D., PICKARD ., Chris, J., Matt, I. J.*Zeitschrift für Kristallographie - Crystalline Materials***2005** , *220* (5/6), 567-570.

46. Stacey, F. D., Brennan, B. J., Irvine, R. D. *Geophysical Surveys***1981** , *4* (3), 189-232.

47. Klapproth, E. G. *Can. J. Phys.* **2003** , *81* (1-2), 503-518.

48. Shimizu, H., Kumazaki, T., Kume, T., Sasaki, S. *Physical Review B Condensed Matter* **2002** , *65* (21), 392-397.